



## Thermo Physical Aspects of Three Dimensional Non-Newtonian $Fe_3O_4/Al_2O_3$ Water Based Hybrid Nanofluid with Rotational Flow over a Stretched Plate

Hussain Shaik<sup>1</sup>, Deepthi Varagani Venkata Lakshmi<sup>2</sup>, Omeshwar Reddy Vulupala<sup>3</sup>, Raghunath Kodi<sup>4</sup>, Giulio Lorenzini<sup>5\*</sup>

<sup>1</sup> Department of Mechanical Engineering, Malla Reddy Engineering College, Medchal-Malkajgiri 500100, India

<sup>2</sup> Department of Mathematics, CVR College of Engineering, Hyderabad 501506, India

<sup>3</sup> Department of Mathematics, Chaitanya Bharathi Institute of Technology, Hyderabad 500075, India

<sup>4</sup> Department of Humanities and Sciences, St. Johns College of Engineering and Technology, Yemmiganur 518360, India

<sup>5</sup> Department of Engineering and Architecture, University of Parma, Parco Area delle Scienze, Parma 43124, Italy

Corresponding Author Email: [Giulio.lorenzini@unipr.it](mailto:Giulio.lorenzini@unipr.it)

Copyright: ©2025 The authors. This article is published by IETA and is licensed under the CC BY 4.0 license (<http://creativecommons.org/licenses/by/4.0/>).

<https://doi.org/10.18280/ijht.430108>

### ABSTRACT

**Received:** 7 December 2024

**Revised:** 20 January 2025

**Accepted:** 5 February 2025

**Available online:** 28 February 2025

#### Keywords:

*hybrid nanofluid, Hall current, 3D flow*

In this paper investigated the three dimensions investigates the effects of a Activation energy and Hall current, along with nonlinear thermal radiation, on a rotating hybrid  $Fe_3O_4/Al_2O_3$  nanofluid over-stretched plate in the presence of a chemical reaction. The main focus of this research is on the implications of these factors. The governing partial differential equations are transformed into nonlinear ordinary differential equations using similarity transformations. The shooting technique is used to generate numerical solutions for that system of equations. Different entrance parameters' effects on the transversal and longitudinal velocities, temperature, heat flow, and surface shear stress are explored numerically and visually. It was shown that there is a strong connection between the primary research and looking at particular situations that indicate how the current technique meets the convergence requirements. In addition, the physical relevance of the contributed parameters is shown via graphs and tables. The discovery demonstrates that an increase in the particle concentration of the hybrid nanofluid accelerates the flow of the fluid. In addition, incorporating dissipative heat makes it more likely that the fluid temperature will be increased to account for the participation of the particle concentration.

## 1. INTRODUCTION

Due to the wide variety of applications in fields such as biomedicine, heat exchangers, cooling of electrical devices, double pane windows, food, and transportation, amongst other areas, the concept of nanofluids have become a more general area of research for scientists in recent years. This is because nanofluids have become more prevalent in recent years. To increase the thermal conductivity of base fluids like ethylene glycol, water, kerosene, and motor oils, it is required to add nanoparticles to these base fluids. Examples of these base fluids include. Graphene, silica, silver, gold, copper, alumina, carbon nanotubes, and other chemically and structurally similar compounds are all examples of nanoparticles. Nanoparticles such as this may vary anywhere from one nanometer to one hundred nanometers in diameter. Choi and Eastman [1] was the first person to make the ground-breaking discovery that nanoparticles floating in a base fluid could increase the thermal conductivity of the liquid, which in turn boosted the fluid's heat transfer rate. This discovery is one of the most important scientific breakthroughs in recent history. Subsequently, Buongiorno [2] investigated the factors that impacted the thermal conductivity of nanofluids and discovered that Brownian motion and the thermophoresis

effect improve the thermal conductivity of nanofluids. This led to the conclusion that Brownian movement and the thermophoresis effect are responsible for the improved thermal conductivity of nanofluids. As a direct consequence of the revelation, Nield and Kuznetsov [3] investigated the boundary layer stream using Buongiorno's model. Khan and Pop [4] were the first researchers to examine the steady flow of nanofluid on a stretched sheet while using convective boundary conditions. Shi et al. [5] investigated the bio-convection flow of magneto-cross nanofluid by using an effective method based on the Prandtl number. The nanofluid included microorganisms. Varun Kumar et al. [6] examined the Arrhenius activation energy for hybrid nanofluid flow across a curved stretching surface. Their findings were published in the journal *Nanoscale*. Shah et al. [7] used the Prandtl hybrid nanofluid flow to examine the effects of bio-convection. Their flow model incorporated both chemical processes and mobile microorganisms. Faraz et al. [8] looked into the multi-slip phenomena that occur during axisymmetric Casson fluid flow using a chemical process.

Arshad and Hassan [9] did some computational research on the flow of hybrid nanofluids through a permeable stretched surface while considering the magnetic field. Hassan et al. [10] investigated viscosity dissipation and heat absorption via the

use of chemical processes and heat sources and sinks. The consequences of chemical reactions and the transmission of melting heat were investigated by Krishnamurthy et al. [11] for the border layer slip flow. Because of its exceptional thermophysical qualities, a recently discovered kind of fluid known as a hybrid nanofluid is finding extensive use in the technological world, and adding two or more nanoparticles to base fluid results in the creation of hybrid nanofluids, which are a kind of advanced fluid. Nanofluids of these types exhibit more advanced characteristics than those of typical nanofluids. A single substance may only have some of the required elements; as a result, the importance can be lacking in certain qualities or characteristics. Other types of nanofluids are less efficient than customizable hybrid nanoparticles when it comes to processing crucial information. When it comes to heat transfer applications, hybrid nanofluids routinely outperform nanofluids. Because of this, they are well suited for application in a wide range of sectors, including biomedicine, refrigeration, cooling electronics, drug reduction, generator cooling, machining coolant, cooling for nuclear systems, and cooling for transformers, amongst a significant number of others. Sunder et al. [12] recently presented a comprehensive method for producing hybrid nanofluids, including the benefits and drawbacks associated with their use. Waini et al. [13] looked into the unsteady flow of a hybrid nanofluid by adding Cu nanoparticles to an Al<sub>2</sub>O<sub>3</sub>/water nanofluid. This nanofluid was formed by inserting the nanoparticles. This uneven flow was generated by a sheet that was stretching and decreasing. Lund et al. [14] discovered that their problem consists of copper, aluminum oxide, and water as the base fluid via numerically calculating the MHD hybrid nanofluid flow toward the decreasing surface for stability analysis and dual solutions. They discovered that when the values of the suction and radiation parameters were increased, the temperature would either increase or drop depending on the solution. Shoaib et al. [15] investigated the phenomenon of viscous dissipation using a spinning disk during 3D MHD hybrid nanofluid flow. According to this body of study, the magnetic field was able to lower the radial and the azimuthal skin friction coefficients. The research done by Ahmad et al. [16] on the use of gold (Go) and silver (Ag) in Maxwell hybrid nano liquid to increase thermal performance was brought to our attention. Their final comments demonstrated that the heat transition might be enhanced by combining a volume proportion of silver with graphene oxide. Alhussain and Tassaddiq [17] investigated the effect of varying consistency on a blood-founded, bi-dimensional Casson hybrid nanofluid by passing it via a stretching sheet while simultaneously adding a magnetic lot perpendicular to the flow domain. Based on this study, the scientists have established that a rise in the concentration of the nanomaterials in the base liquid causes an increase in the thermal expansion rate while simultaneously causing a reduction in the specific heat capacity.

People have paid more attention to how thermal radiation affects natural convection in recent years. This is because thermal radiation has many uses in engineering and physics, especially in making instruments and equipment, aeronautical engineering, and gas turbines. Thermal radiation is the most desirable way of heat transfer since it does not need a medium for its operation. This makes it superior to conduction and convection. Due to these properties, thermal radiation plays an essential part in the heat transfer of MHD nanofluids, which helps keep the amount of heat lost to a minimum. Radiation parameters are among the most crucial components for

controlling the flow of liquid and heat in a high-temperature heat system. Thermal radiation has significantly influenced the development of many modern transformation systems and steady-state equipment, such as missiles and satellites, nuclear power plants, gas turbines, and nuclear power plants. The consequence of Hall wind and joule heating on a rotating hybrid nanofluid over an extended vessel with nonlinear thermal radiation was dissected by Elsaid and AlShurafat [18]. In the beginning, England and Emery [19] investigated heat radiation's influence on the laminar flow of air and carbon dioxide as it passed through a vertical plate. Elsaid and Abdel-Wahed [20] researched MHD composite convection Ferro Fe<sub>3</sub>O<sub>4</sub>/Cu-hybrid-nanofluid flows in a steep channel to learn more about the phenomenon. A model to mimic the flow and heat transfer of a nanofluid over an infinite vertical plate while exposed to a magnetic field and viscous dissipation was created by Kumar et al. [21]. In a further study, Ali et al. [22] investigated how thermal radiation affected the flow of MHD hybrid nanofluid along the stretched cylinder. Specifically, they were interested in how the radiation affected the flow. The influence of thermal radiation, Hall current, and unequal heat source/sink on the nanofluid flow between two horizontal flat plates was studied by Lv et al. [23] in a scenario in which the bottom plate was stretch permeable. The influence of heat radiation and chemical response on MHD Casson nanofluid gush induced owing to a stretched sheet was investigated by Rao and Deka [24]. Rao and Deka [25] conducted a numerical analysis of a nanofluid's heat and mass transport phenomena when it was recently subjected to solar radiation's influence. Imagine a fluid that is rotating and stable, laminar, and incompressible. This fluid also has a constant angular velocity, including electrically conducting Fe<sub>3</sub>O<sub>4</sub>/Al<sub>2</sub>O<sub>3</sub> hybrid nanoparticles moving at a uniform velocity  $U_w = bx$  across a stretched plate.

The primary intent of this study is to investigate the steady outpour of laminar, incompressible, hybrid nanofluid beyond a stretchy, rotating dish utilizing a Hall current, Joule heating, and chemical reaction utilizing hybrid nanoparticles of Fe<sub>3</sub>O<sub>4</sub> and Al<sub>2</sub>O<sub>3</sub> while being subjected to the effects of a magnetic field. Both the liquid and the plates are moving in the same direction at the same consistent speed around the axis of the trajectory. The equations that determine momentum, energy, and concentration are converted into ordinary differential equations (ODEs) using a similarity transformation. Then the boundary value problem method is used to solve the ODEs in MATLAB. The impact of various restrictions is broken down and analyzed using graphical representations and tabular data.

## 2. FLOW GOVERNING EQUATIONS

Consider a rotating fluid that is steady–laminar–incompressible and has a constant angular velocity and contains electrically conducting Fe<sub>3</sub>O<sub>4</sub>/Al<sub>2</sub>O<sub>3</sub> hybrid nanoparticles traveling at a uniform velocity  $U_w = bx$  over a stretched plate. Nonlinear thermal radiation with heat flux  $q_r = \frac{-4\sigma^*}{3\alpha^*} \left( \frac{\partial T^4}{\partial z} \right)$ , uniform magnetic fields of intensity  $B_0$  and Hall current are applied to the plate in a normal direction. The temperature on the surface is  $T_w$ , whereas  $T_\infty$  is the temperature away from the surface. The geometry of the problem is shown in Figure 1. The equations describing the model are presented in the study by Elsaid and AlShurafat [18].

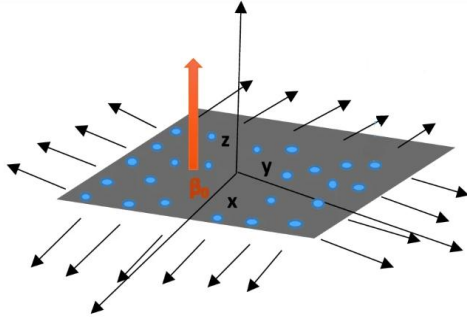


**Figure 1.** Schematic representation of the physical space including the coordinate system

$$\frac{\partial u}{\partial x} + \frac{\partial v}{\partial y} + \frac{\partial w}{\partial z} = 0 \quad (1)$$

$$\rho_{hnf} \left( u \frac{\partial u}{\partial x} + v \frac{\partial u}{\partial y} + w \frac{\partial u}{\partial z} - 2\omega v \right) = \mu_{hnf} \frac{\partial^2 u}{\partial z^2} - \frac{\sigma_{hnf} B_0^2}{(1+m^2)} (u - mv) \quad (2)$$

$$\rho_{hnf} \left( u \frac{\partial v}{\partial x} + v \frac{\partial v}{\partial y} + w \frac{\partial v}{\partial z} + 2\omega u \right) = \mu_{hnf} \frac{\partial^2 v}{\partial z^2} - \frac{\sigma_{hnf} B_0^2}{(1+m^2)} (v + mu) \quad (3)$$

$$\left( \rho C_p \right)_{hnf} \left( u \frac{\partial T}{\partial x} + v \frac{\partial T}{\partial y} + w \frac{\partial T}{\partial z} \right) = k_{hnf} \left( \frac{\partial^2 T}{\partial z^2} \right) + \frac{\partial^2 T^4}{\partial z^2} \left( \frac{4\sigma^*}{3\alpha^*} \right) + Q_0 (T - T_\infty) + \sigma_{hnf} B_0^2 (u^2 + v^2) \quad (4)$$

$$u \frac{\partial C}{\partial x} + v \frac{\partial C}{\partial y} + w \frac{\partial C}{\partial z} = \beta_{hnf} \left( \frac{\partial^2 C}{\partial z^2} \right) - k_r^2 (C - C_\infty) \left( \frac{T}{T_\infty} \right)^m \exp \left( \frac{-E_a}{K^* T} \right) \quad (5)$$

For this flow, corresponding boundary conditions are [18]:

$$\begin{aligned} u \rightarrow 0, v \rightarrow 0, w \rightarrow 0, T \rightarrow T_\infty, C \rightarrow C_\infty \text{ as } z \rightarrow \infty \\ u = U_w, v = 0, w = 0, T = T_w, C = C_w \text{ at } z = 0 \end{aligned} \quad (6)$$

The effective properties of hybrid nanofluid are given by Elsaid and AlShurafat [18], and Elsaid and Abdel-Wahed [20]:

$$\begin{aligned} \frac{\mu_{hnf}}{\mu_f} &= \left( \frac{1}{(1-\phi_2)^{2.5} (1-\phi_1)^{2.5}} \right), \\ \rho_{hnf} &= (1-\phi_2) \left[ (1-\phi_2) \rho_f + \phi_1 \rho_{s1} \right] + \phi_2 \rho_{s2}, \\ \left( \rho C_p \right)_{hnf} &= (1-\phi_2) \left[ (1-\phi_2) \left( \rho C_p \right)_f + \phi_1 \left( \rho C_p \right)_{s1} \right] + \phi_2 \left( \rho C_p \right)_{s2}, \\ k_{nf} &= k_f \left( \frac{k_{s1} + 2k_{nf} - 2\phi_1 (k_{nf} - 2k_{s1})}{k_{s1} + 2k_{nf} + 2\phi_1 (k_{nf} - 2k_{s1})} \right), \\ k_{hnf} &= k_{nf} \left( \frac{k_{s2} + 2k_{nf} - 2\phi_2 (k_{nf} - 2k_{s2})}{k_{s2} + 2k_{nf} + 2\phi_2 (k_{nf} - 2k_{s2})} \right), \\ \sigma_{nf} &= \sigma_f \left( \frac{\sigma_{s1} + 2\sigma_{nf} - 2\phi_1 (\sigma_{nf} - 2\sigma_{s1})}{\sigma_{s1} + 2\sigma_{nf} + 2\phi_1 (\sigma_{nf} - 2\sigma_{s1})} \right), \end{aligned}$$

$$\sigma_{hnf} = \sigma_{nf} \left( \frac{\sigma_{s2} + 2\sigma_{nf} - 2\phi_2 (\sigma_{nf} - 2\sigma_{s2})}{\sigma_{s2} + 2\sigma_{nf} + 2\phi_2 (\sigma_{nf} - 2\sigma_{s2})} \right),$$

Here,  $\phi_1, \phi_2$  are the solid volume fractions of  $\text{Fe}_3\text{O}_4$  and  $\text{Al}_2\text{O}_3$  respectively, subscript  $s_1, s_2, f$ , and  $hnf$  are for nano-solid-particles, base fluid, and hybrid nanofluid respectively. As shown in Table 1.

**Table 1.** Thermo-physical possessions of  $\text{H}_2\text{O}$ ,  $\text{Fe}_3\text{O}_4$ , and  $\text{Al}_2\text{O}_3$  followed by [18, 20]

Physical Properties	Water	$\text{Fe}_3\text{O}_4$	$\text{Al}_2\text{O}_3$
$C_p$ (J/KgK)	4179	670	765
$\rho$ (Kg/m <sup>3</sup> )	997.1	5180	3970
$k$ (w/mK)	0.613	9.7	40
$\sigma$ ( $\Omega$ /m)	$25 \cdot 10^{-2}$	$25 \cdot 10^3$	$35 \cdot 10^6$

By adding the following similarity transformation, which is utilized to change the dimensionless PDEs into the dimensionless odes, dimensional quantities are provided to simplify the mathematical analysis of the issue.

$$\begin{aligned} u &= bx f'(\eta), v = by g(\eta), \\ w &= -\sqrt{b\nu_f} (f(\eta) + g(\eta)), T = T_\infty + \Delta T \theta(\eta), \\ \eta &= \sqrt{\frac{b}{\nu_f}} z, \theta(\eta) = \frac{T - T_\infty}{T_w - T_\infty}, \phi(\eta) = \frac{C - C_\infty}{C_w - C_\infty} \end{aligned} \quad (7)$$

The subsequent set of non-linear ordinary differential equations is conveyed by plugging Eq. (7) into Eqs. (2), (3), and (4):

$$\begin{aligned} \left( \frac{l_4}{l_1} \right) f''' - f'^2 + ff'' + 2\lambda g - \\ \left( \frac{l_5}{l_1} \right) \frac{M}{(1+m^2)} (f' - mg) = 0 \end{aligned} \quad (8)$$

$$\begin{aligned} \left( \frac{l_4}{l_1} \right) g'' + fg' - f'g - 2\lambda f' - \\ \left( \frac{l_5}{l_1} \right) \frac{M}{(1+m^2)} (g + mf') = 0 \end{aligned} \quad (9)$$

$$\begin{aligned} \theta'' + \left( \frac{R_d}{l_3} \right) [(1 + (\theta_w - 1)\theta)]^3 \theta'' + \\ \text{Pr} \left( \frac{l_2}{l_3} \right) f\theta' + \left( \frac{3R_d}{l_3} \right) \times (\theta_w - 1) \\ [(1 + (\theta_w - 1)\theta)]^2 \theta'^2 + \text{Pr} Ec M \left( \frac{l_5}{l_3} \right) \times \\ (f'^2 + g'^2) + \text{Pr} Q \theta = 0 \end{aligned} \quad (10)$$

$$\begin{aligned} \phi'' + \frac{Sc}{(1-\phi_1)(1-\phi_2)} (f + g)\phi' - \\ K_E (1 + \theta)^m \phi \exp \left( \frac{-E}{1 + \theta} \right) = 0 \end{aligned} \quad (11)$$

where, the prime conveys differentiation with consideration to  $(\eta)$  and it is given by  $\phi_2$ .

$$l_1 = \frac{\rho_{hnf}}{\rho_f}, l_2 = \frac{(\rho C_p)_{hnf}}{(\rho C_p)_f}, l_3 = \frac{k_{hnf}}{k_f}, l_4 = \frac{\mu_{hnf}}{\mu_f}, \text{ and } l_5 = \frac{\sigma_{hnf}}{\sigma_f}.$$

The modified boundary conditions corresponding to the transformation (5) are then:

$$\begin{aligned} f(\eta) &= 0, g(\eta) = 0, f'(\eta) = 1, \theta(\eta) = 0, \phi(\eta) = 1 \text{ at } \eta = 0 \\ f'(\eta) &\rightarrow 0, g(\eta) \rightarrow 0, \theta(\eta) \rightarrow 0, \phi(\eta) \rightarrow 0 \text{ as } \eta \rightarrow \infty \end{aligned} \quad (12)$$

where, "prime" stands for "differentiation with regard to  $\eta$ " and "defines" the important thermophysical parameters that indicate the flow dynamics.

$$\left\{ \begin{aligned} \lambda &= \frac{\omega}{b}, M = \frac{\sigma_f B_0^2 x}{\rho_f b}, Pr = \frac{\nu_f}{k_f} = \frac{(\nu \rho C_p)_f}{k_f}, \\ \theta_w &= \frac{T_w}{T_\infty}, Ec = \frac{u^2 \rho_f}{(\rho C_p)_f (T_w - T_\infty)}, Sc = \frac{\nu_f}{\beta_f} \\ R_d &= \frac{16 \sigma^* T_\infty^3}{3 k_f \alpha^*}, K_r = \frac{\xi_1 k_T (C - C_\infty)^{n-1}}{b}, \\ Q &= \frac{Q_0}{(\rho C p)_f k_f}, K_E = \frac{k_r^2}{c}, E = \frac{E_a}{K^* T_\infty}. \end{aligned} \right. \quad (13)$$

### 3. PHYSICAL QUANTITIES OF INTERESTS

The physical quantities of the given problem are, the "Skin friction" along x and y axis  $Cf_x$ ;  $Cf_y$ , the "local Nusselt number"  $Nu_x$  and the "Sherwood number"  $Sh_x$ , defined by:

$$\begin{aligned} Cf_x &= \frac{\mu_{hnf}}{\rho_f (bx)^2} \left( \frac{\partial u}{\partial z} \right)_{z=0}, Cf_y = \frac{\mu_{hnf}}{\rho_f (bx)^2} \left( \frac{\partial v}{\partial z} \right)_{z=0}, \\ Nu_x &= -\frac{x k_{hnf}}{k_f (T_w - T_\infty)} \left( \frac{\partial T}{\partial z} \right)_{z=0}, Sh_x = -\frac{x k_{hnf}}{k_f (C_w - C_\infty)} \left( \frac{\partial C}{\partial z} \right)_{z=0} \end{aligned} \quad (14)$$

**Table 2.** Comparison of  $f''(0)$ ,  $g'(0)$  with a previous studied when  $M=m=Ec=\phi_1=\phi_2=Sc=Rc=0$ ,  $E=0$ ,  $Q=0$

	Elsaid and Abdel-Wahed [20]		Elsaid and AlShurafat [18]		Current Study	
$\Lambda$	$f''(0)$	$g'(0)$	$f''(0)$	$g'(0)$	$f''(0)$	$g'(0)$
0.5	-1.14383	-0.51277	-1.14383	-0.515276	-1.154263	-0.540253
1.0	-1.325505	-0.83715	-1.32450	-0.837510	-1.325236	-0.834474
2.0	-1.622535	-1.28724	-1.65243	-1.287256	-1.642536	-1.247458

**Table 3.** Comparison of  $NuR_e^{-1/2}$  with a previous studied when  $M=1$ ,  $Ec=E=Q=0$ ,  $\phi_1=0.1$ ,  $\phi_2=0$ ,  $\lambda=0.5$ ,  $Sc=Rc=0$

Rd	$\Theta_w$	Elsaid and Abdel-Wahed [20]	Elsaid and AlShurafat [18]	Current Study
0	1	1.85750	1.835750	1.825277
1	1	2.234679	2.234679	2.244688
1	1.1	2.304471	2.304571	2.347686
1	1.5	2.608856	2.608665	2.636387

In terms of the similarity variable, the following is an articulation of the coefficient of skin friction, the Nusselt numeral, and the Sherwood numeral in their non-dimensional structures:

$$\begin{aligned} Re_x^{1/2} Cf_x &= \frac{\mu_{hnf}}{\mu_f} f''(0), Re_x^{1/2} Cf_y = \frac{\mu_{hnf}}{\mu_f} g''(0), \\ Re_x^{-1/2} Nu_x &= -\left( \frac{k_{hnf}}{k_f} + Rd \theta_w^3 \right) \theta'(0), \\ Re_x^{-1/2} Sh_x &= -\frac{k_{hnf}}{k_f} \phi'(0) \end{aligned} \quad (15)$$

### 4. METHOD OF SOLUTION

The group of nonlinear connected ordinary differential Eqs. (7)-(10) has been solved numerically using the Runge-Kutta fourth-order method combined with a shooting approach, utilizing MATLAB software with a step size of  $\Delta\eta=0.01$  and an error bound of  $10^{-6}$  in all cases. By introducing additional variables, the connected nonlinear ODEs are transformed into a set of linear first-order ODEs, which is one of the advantages of this technique. Additionally, the boundary value problem is converted into an initial value problem by assigning guess values to the unknown starting values based on the parameters that need to be addressed. The shooting method then adjusts these estimated values to align them with the boundary conditions established for the other boundary. After the necessary number of iterations to correct the estimated values, forward integration is performed to provide numerical solutions for the requested locations and intervals.

The following are the limitations: "not" II PDEs representing the governing equations can be transformed using similarity transformations and, therefore, cannot be converted into ODEs. Only certain categories of flow problems are suitable candidates for similarity transformations and comparable solutions. Additionally, a particular issue may have more than one solution, in which case it is necessary to select the most reliable solution and discuss the reasons. The numerical values of the variables are shown in Tables 2 and 3, respectively, to evaluate the correctness of the current code and perform a validity check.

In conclusion, the results of the numerical simulations for the rate coefficients, including the shear rate and the heat transfer rate, showing the impact of various contributing factors. It has been demonstrated that increased values of nanoparticle concentration, magnetic parameter, and thermal buoyancy significantly enhance the rate of shear stress. Furthermore, the nanoparticle concentrations of both  $Fe_3O_4$  and  $Al_2O_3$  increase the magnitude of the heat transfer rate, although other contributing factors have a retarding effect on the heat transfer rate profile.

## 5. DISCUSSION OF THE RESULT

A boundary layer is modeled over a stretched plate involving a spinning hybrid nanofluid. Water is used as the base fluid, with  $Fe_3O_4$  and  $Al_2O_3$  nanoparticles included. The effects of a magnetic field, Hall current, rotation parameter, chemical reaction, and nonlinear thermal radiation on the boundary layer were explored using figures numbered 2 to 15. While calculating velocity, the x-axis determines the longitudinal component, and the y-axis calculates the transversal component. The following section discusses the findings.

The effect of the magnetic field, represented by the Hartman number ( $M$ ), is shown in Figure 2. An increase in the Hartman number results in a decrease in velocity in both the x and y directions. The magnetic field thins the boundary layer, reducing the fluid's capacity to travel in both directions. A dashed line in the illustrations indicates the presence of a Hall current along with the magnetic field. While the Hall current did not visibly affect the longitudinal velocity, it did increase the transversal velocity. Figure 3 shows that this rise in transversal velocity is more pronounced when magnetic strength is increased. The Hall current in a region influenced by a magnetic field generates a Lorentz force, a drag force acting perpendicularly, forcing the fluid molecules to change direction and increasing the transversal velocity. Figure 4 illustrates how a magnetic field can affect temperature profiles, causing fluid molecules near the surface to migrate and raise the boundary layer's temperature. The Hall current increases the thermal boundary layer thickness and temperature due to Joule heating induced by the intense magnetic field.

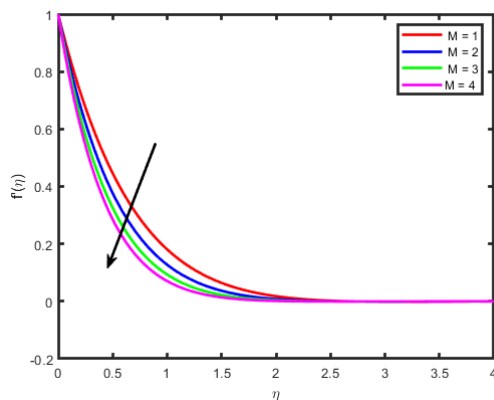


Figure 2. Impact of  $M$  on  $f'(\eta)$

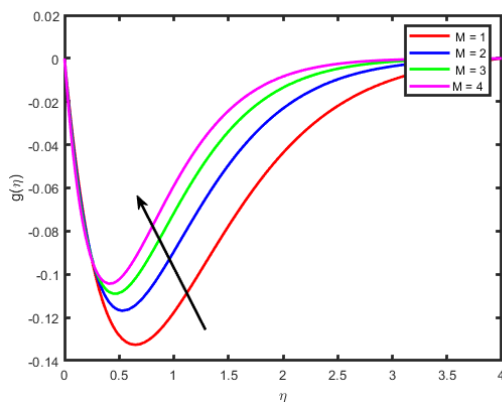


Figure 3. Impact of  $M$  on  $g(\eta)$

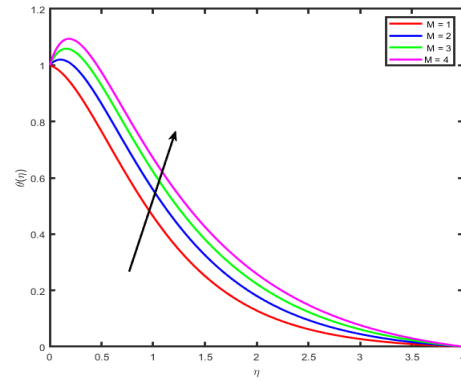


Figure 4. Impact of  $M$  on  $\theta(\eta)$

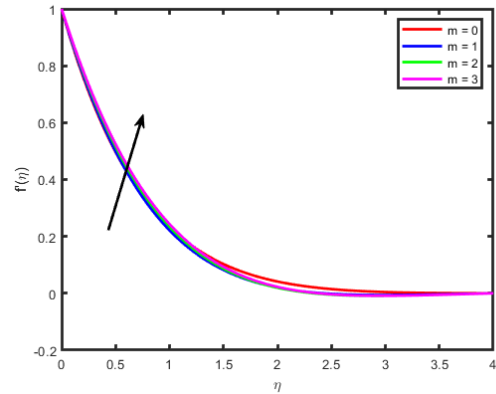


Figure 5. Impact of  $M$  on  $f'(\eta)$

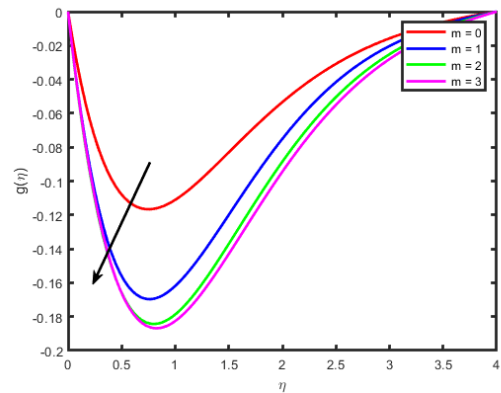


Figure 6. Impact of  $M$  on  $g(\eta)$

Figures 5 and 6 show the effects of the Hall current parameter ( $M$ ) on the longitudinal and transversal velocity profiles, respectively. An increase in the Hall current parameter causes a rise in longitudinal velocity in fluid velocity (Figure 5), and the transversal velocity decreases (Figure 6). Figure 7 displays the impact of the rotation parameter ( $\Lambda = \Omega/B$ ) on longitudinal velocity, indicating that a higher rotation parameter value suggests a stronger rotation rate, leading to increased centrifugal force and speeding up fluid particles in the radial direction. Figure 8 depicts how increasing the rotation parameter also increases the transversal velocity. Figures 9 and 10 show that an increase in the rotation parameter leads to a drop in the hybrid nanofluid's temperature and concentration fields. Figures 11 and 12 illustrate the effect of the radiation parameter ( $Rd$ ) on temperature and concentration profiles. An increase in the radiation parameter results in a temperature rise due to increased thermal radiation releasing heat energy into the fluid. The temperature profile of the hybrid nanofluid is greater than that of the standard nanofluid, while the concentration field shows the opposite

behavior. Figure 13 demonstrates that an increase in the Eckert number ( $E_c$ ) causes a rise in the temperature field, explained by the transformation of kinetic energy into thermal energy. Figure 14 shows the effect of the chemical reaction parameter ( $R_c$ ) on the concentration profile, with an increase in  $R_c$  decreasing the concentration boundary layer thickness. Figure 15 illustrates the Schmidt number's influence on the concentration profile, showing a relationship between the diffusivity of momentum and mass, with higher Schmidt numbers leading to lower concentration profiles and thinner boundary layers for hybrid nanofluids with pure and mixed nanoparticles.

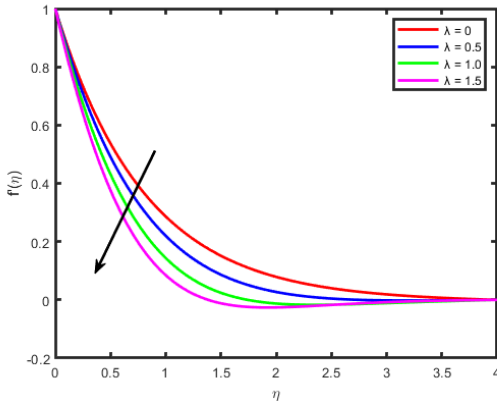


Figure 7. Impact of  $\Lambda$  on  $f'(\eta)$

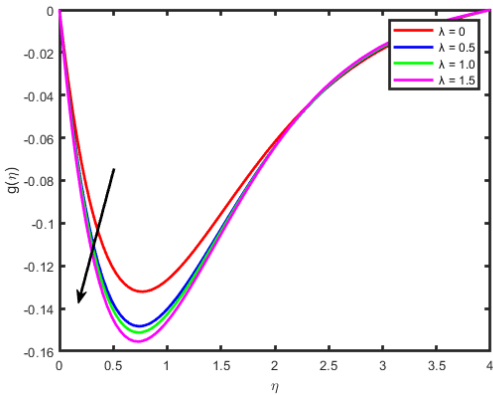


Figure 8. Impact of  $\Lambda$  on  $g(\eta)$

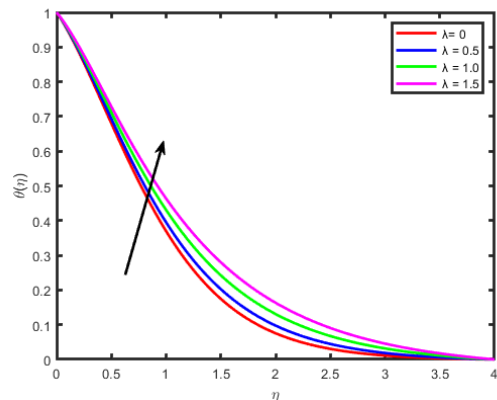


Figure 9. Impact of  $\Lambda$  on  $\theta(\eta)$

Figure 16 demonstrates a correlation between increased heat source/sink resistance and temperature rise. Conversely, Figure 17 shows the opposite behavior under focus conditions. Figure 18 illustrates the influence of activation energy ( $E$ ) on the concentration field, showing that higher  $E$  values increase the concentration profile due to the generative chemical reaction encouraged by the Arrhenius function's degradation.

Higher activation energy and lower temperatures result in a slower chemical reaction rate, leading to increased concentration. Figure 19 shows that an increase in the chemical reaction rate ( $\Sigma$ ) significantly decreases the concentration profile, with a high reaction rate causing a denser solute boundary layer.

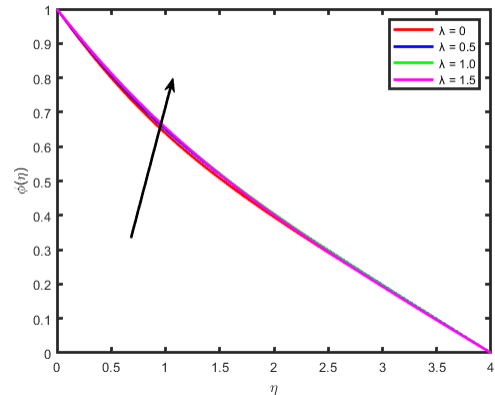


Figure 10. Impact of  $\Lambda$  on  $\varphi(\eta)$

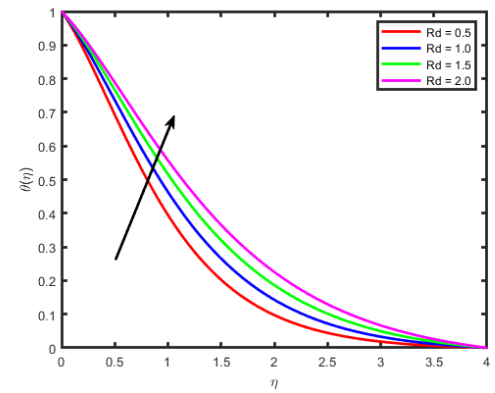


Figure 11. Impact of  $R_a$  on  $\theta(\eta)$

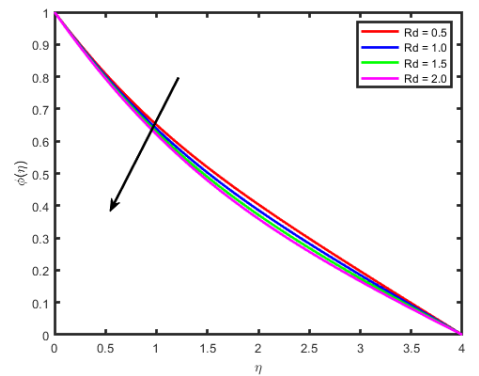


Figure 12. Impact of  $R_a$  on  $\varphi(\eta)$

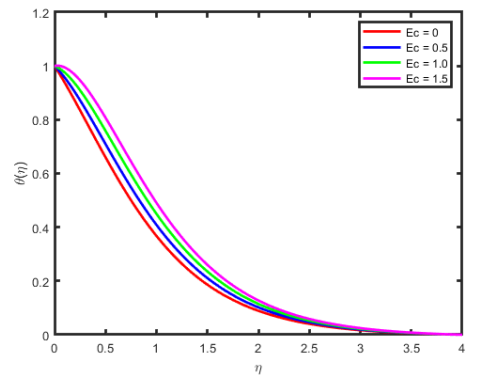
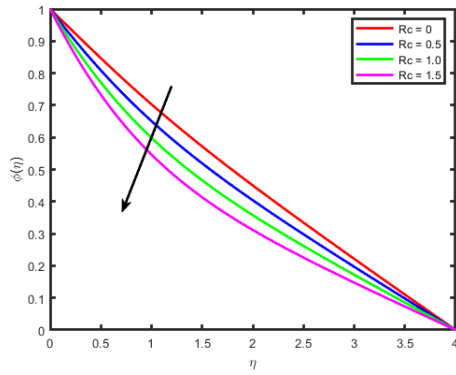
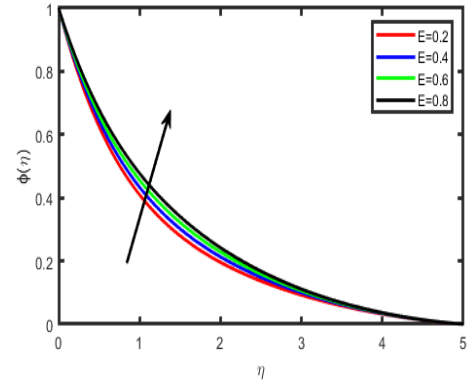


Figure 13. Impact of  $E_c$  on  $\theta(\eta)$



**Figure 14.** Impact of  $R_c$  on  $\varphi(\eta)$



**Figure 18.** Effect of  $E$  on  $\varphi(\eta)$

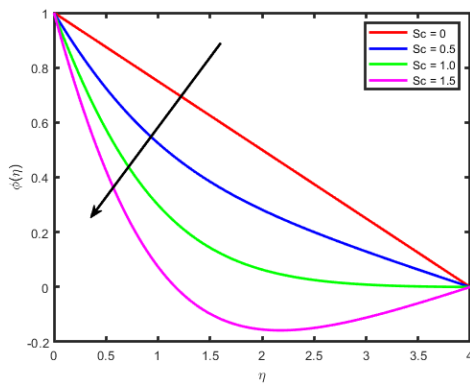


**Figure 15.** Impact of  $S_c$  on  $\varphi(\eta)$

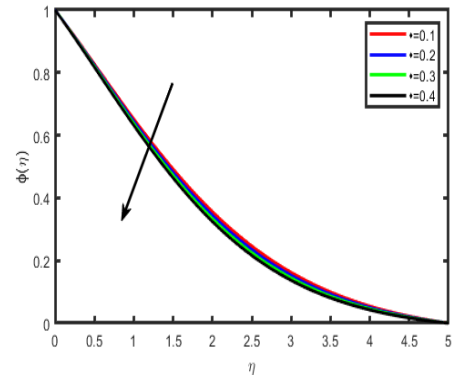


**Figure 19.** Effect of  $\sigma$  on  $\varphi(\eta)$

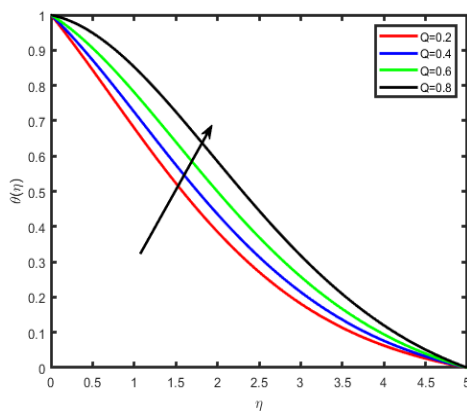


**Figure 16.** Effect of  $Q$  on  $\varphi(\eta)$

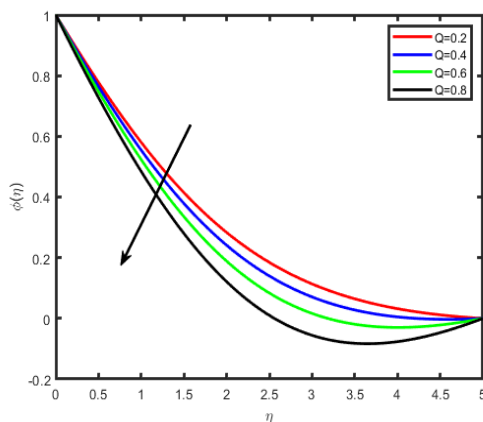


**Figure 17.** Effect of  $Q$  on  $\varphi(\eta)$

## 6. CONCLUSION

This work presented a mathematical simulation to study the impact of Hall current, magnetic field, joule heating, rotation parameter, and nonlinear thermal radiation on a rotating hybrid  $Fe_3O_4/Al_2O_3$  nanofluid over-stretched plate using a set of governing partial differential equations. The system transformed to be dimensionless one dimension of a single variable and then solved numerically with a mix of find root and Runge Kutta method to overcome the missing of the boundary conditions. The following are the most important aspects of this research.

- An increment in the magnetic parameter  $M$  diminishes the velocity of the hybrid nanofluid, but at the same time, causing enhances in the profile of  $(\eta)$ , temperature and concentration of the hybrid nanofluid.
- When the rotation parameter is present the longitudinal velocity decreases while the transverse velocity increases and the temperature of a boundary layer rise as the kinetic energy of the fluid increases. When a boundary layer is exposed to thermal radiation, it has a higher temperature than when it isn't.
- Because the fluid viscosity rises when a dual-type of the nanoparticle is used, the velocity decreases more rapidly.

The propose study brings a road way to analyze the physical behaviour of the various nanoparticles on the hybrid nanofluid flow and their real-life applications in industries as well as engineering. In a broad sense, cooling is one of the important applications where the range of the temperature is high. For example, refrigeration as well as the ventilation, and air conditioning applications are commonly used.

## REFERENCES

- [1] Choi, S.U.S., Eastman, J.A. (1995). Enhancing thermal conductivity of fluids with nanoparticles. ASME International Mechanical Engineering Congress and Exposition, 66: 99-105.
- [2] Buongiorno, J. (2006). Convective transport in nanofluids. *Journal of Heat Transfer*, 128(3): 240-250.
- [3] Nield, D.A., Kuznetsov, A.V. (2009). Thermal instability in a porous medium layer saturated by a nanofluid. *International Journal of Heat and Mass Transfer*, 52(25-26): 5796-5801. <https://doi.org/10.1016/j.ijheatmasstransfer.2009.07.023>
- [4] Khan, W.A., Pop, I. (2010). Boundary-layer flow of a nanofluid past a stretching sheet. *International Journal of Heat and Mass Transfer*, 53(11-12): 2477-2483. <https://doi.org/10.1016/j.ijheatmasstransfer.2010.01.032>
- [5] Shi, Q.H., Hamid, A., Khan, M.I., Kumar, R.N., Gowda, R.P., Prasannakumara, B.C., Shah, N.A., Khan, S.U., Chung, J.D. (2021). Numerical study of bio-convection flow of magnetocross nanofluid containing gyrotactic microorganisms with effective. *Scientific Reports*, 11: 16030. <https://doi.org/10.1038/s41598-021-95587-2>
- [6] Varun Kumar, R.S., Alhadhrami, A., Punith Gowda, R.J., Naveen Kumar, R., Prasannakumara, B.C. (2021). Exploration of Arrhenius activation energy on hybrid nanofluid flow over a curved stretchable surface. *Journal of Applied Mathematics and Mechanics*, 101(12): e202100035. <https://doi.org/10.1002/zamm.202100035>
- [7] Shah, S.A.A., Ahammad, N.A., Din, E.M.T.E., Gamaoun, F., Awan, A.U., Ali, B. (2022). Bio-convection effects on prandtl hybrid nanofluid flow with chemical reaction and motile microorganism over a stretching sheet. *Nanomaterials*, 12(13): 2174. <https://doi.org/10.3390/nano12132174>
- [8] Faraz, F., Imran, S.M., Ali, B., Haider, S. (2019). Thermo-diffusion and multi-slip effect on an axisymmetric Casson flow over a unsteady radially stretching sheet in the presence of chemical reaction. *Processes*, 7(11): 851. <https://doi.org/10.3390/pr7110851>
- [9] Arshad, M., Hassan, A. (2022). A numerical study on the hybrid nanofluid flow between a permeable rotating system. *The European Physical Journal Plus*, 137(10): 1126. <https://doi.org/10.1140/epjp/s13360-022-03313-2>
- [10] Hassan, A., Hussain, A., Arshad, M., Gouadria, S., Awrejcewicz, J., Galal, A.M., Alharbi, F.M., Eswaramoorthi, S. (2022). Insight into the significance of viscous dissipation and heat generation/absorption in magneto-hydrodynamic radiative Casson fluid flow with first-order chemical reaction. *Frontiers in Physics*, 10: 605. <https://doi.org/10.3389/fphy.2022.920372>
- [11] Krishnamurthy, M.R., Gireesha, B.J., Prasannakumara, B.C., Gorla, R.S.R. (2016). Thermalradiation and chemicalreaction effects on boundary layer slip flow and melting heat transfer of nanofluid induced by a nonlinear stretching sheet. *Nonlinear Engineering*, 5(3): 147-159. <https://doi.org/10.1515/nleng-2016-0013>
- [12] Sundar, L.S., Sharma, K.V., Singh, M.K., Sousa, A.C.M. (2017). Hybrid nanofluids preparation, thermal properties, heat transfer and friction factor-A review. *Renew. Sustain. Renewable and Sustainable Energy Reviews*, 68: 185-198. <https://doi.org/10.1016/j.rser.2016.09.108>
- [13] Waini, I., Ishak, A., Pop, I. (2019). Unsteady flow and heat transfer past a stretching/shrinking sheet in a hybrid nanofluid. *International Journal of Heat and Mass Transfer*, 136: 288-297. <https://doi.org/10.1016/j.molliq.2018.04.041>
- [14] Lund, L.A., Omar, Z., Khan, I., Sherif, E.S.M. (2020). Dual solutions and stability analysis of a hybrid nanofluid over a stretching/shrinking sheet executing MHD flow. *Symmetry*, 12(2): 1-14. <https://doi.org/10.3390/sym12020276>
- [15] Shoaib, M., Raja, M.A.Z., Sabir, M.T., Awais, M., Islam, S., Shah, Z., Kumam, P. (2021). Numerical analysis of 3-D MHD hybrid nanofluid over a rotational disk in presence of thermal radiation with Joule heating and viscous dissipation effects using Lobatto IIIA technique. *Alexandria Engineering Journal*, 60(4): 3605-3619. <https://doi.org/10.1016/j.aej.2021.02.015>
- [16] Ahmad, F., Abdal, S., Ayed, H., Hussain, S., Salim, S., Almatroud, A.O. (2021). The improved thermal efficiency of Maxwell hybrid nanofluid comprising of graphene oxide plus silver/kerosene oil over stretching sheet. *Case Studies in Thermal Engineering*, 27: 101257. <https://doi.org/10.1016/j.csite.2021.101257>
- [17] Alhussain, Z.A., Tassaddiq, A. (2022). Thin film blood based casson hybrid nanofluid flow with variable viscosity. *Arabian Journal for Science and Engineering*, 47: 1087-1094. <https://doi.org/10.1007/s13369-021-06067-8>
- [18] Elsaid, E.M., AlShurafat, K.S. (2023). Impact of hall current and joule heating on a rotating hybrid nanofluid over a stretched plate with nonlinear thermal radiation. *Journal of Nanofluids*, 12(2): 548-556. <https://doi.org/10.1166/jon.2023.1927>
- [19] England, W.G., Emery, A.F. (1969). Thermal radiation effects on the laminar free convection boundary layer of an absorbing gas. *ASME Journal of Heat and Mass Transfer*, 91(1): 37-44.
- [20] Elsaid, E.M., Abdel-Wahed, M.S. (2022). MHD mixed convection Ferro  $Fe_3O_4$ /Cu-hybrid-nanofluid runs in a vertical channel. *Chinese Journal of Physics*, 76: 269-282. <https://doi.org/10.1016/j.cjph.2021.12.016>
- [21] Kumar, M.A., Reddy, Y.D., Rao, V.S., Goud, B.S. (2021). Thermal radiation impact on MHD heat transfer natural convective nano fluid flow over an impulsively started vertical plate. *Case Studies in Thermal Engineering*, 24: 100826. <https://doi.org/10.1016/j.csite.2020.100826>
- [22] Ali, A., Kanwal, T., Awais, M., Shah, Z., Kumam, P., Thounthong, P. (2021). Impact of thermal radiation and non-uniform heat flux on MHD hybrid nanofluid along a stretching cylinder. *Scientific Reports*, 11(1): 20262. <https://doi.org/10.1038/s41598-021-99800-0>
- [23] Lv, Y.P., Shaheen, N., Ramzan, M., Mursaleen, M., Nisar, K.S., Malik, M.Y. (2021). Chemical reaction and thermal radiation impact on a nanofluid flow in a rotating channel with Hall current. *Scientific Reports*, 11(1): 19747. <https://doi.org/10.1038/s41598-021-99214-y>
- [24] Rao, S., Deka, P. (2022). A numerical solution using EFDM for unsteady MHD radiative Casson nanofluid flow over a porous stretching sheet with stability analysis. *Heat Transfer*, 51(8): 8020-8042. <https://doi.org/10.1002/htj.22679>
- [25] Rao, S., Deka, P.N. (2022). A numerical investigation on transport phenomena in a nanofluid under the transverse

magnetic field over a stretching plate associated with solar radiation. *Nonlinear Dynamics and Applications*,

473-492. [https://doi.org/10.1007/978-3-030-99792-2\\_39](https://doi.org/10.1007/978-3-030-99792-2_39)